THE JOURNAL OF BIOLOGICAL CHEMISTRY
Vol. 277, No. 26, Issue of June 28, pp. 23604–23611, 2002

Printed in U.S.A.

Loss of Hyperpolarization-activated Cl^- Current in Salivary Acinar Cells from *Clcn2* Knockout Mice*

Received for publication, March 25, 2002, and in revised form, April 18, 2002
Published, JBC Papers in Press, April 25, 2002, DOI 10.1074/jbc.M202900200

Keith Nehrke‡§, Jorge Arreola‡¶, Ha-Van Nguyen‡§, Jodi Pilato‡, Linda Richardson‡, Gbolahan Okunade‖, Raymond Baggs, Gary E. Shull‖, and James E. Melvin‡§‡‡**

*From the ‡Center for Oral Biology, Aab Institute of Biomedical Sciences, the §Eastman Department of Dentistry, the **Department of Laboratory Animal Medicine, and the ¶Department of Pharmacology and Physiology, University of Rochester Medical Center, Rochester, New York 14642 and the ‖Department of Molecular Genetics, Biochemistry, and Microbiology, University of Cincinnati College of Medicine, Cincinnati, Ohio 45267*

ClC-2 is localized to the apical membranes of secretory epithelia where it has been hypothesized to play a role in fluid secretion. Although ClC-2 is clearly the inwardly rectifying anion channel in several tissues, the molecular identity of the hyperpolarization-activated Cl^- current in other organs, including the salivary gland, is currently unknown. To determine the nature of the hyperpolarization-activated Cl^- current and to examine the role of ClC-2 in salivary gland function, a mouse line containing a targeted disruption of the *Clcn2* gene was generated. The resulting homozygous *Clcn2*$^{-/-}$ mice lacked detectable hyperpolarization-activated chloride currents in parotid acinar cells and, as described previously, displayed postnatal degeneration of the retina and testis. The magnitude and biophysical characteristics of the volume- and calcium-activated chloride currents in these cells were unaffected by the absence of ClC-2. Although ClC-2 appears to contribute to fluid secretion in some cell types, both the initial and sustained salivary flow rates were normal in *Clcn2*$^{-/-}$ mice following *in vivo* stimulation with pilocarpine, a cholinergic agonist. In addition, the electrolytes and protein contents of the mature secretions were normal. Because ClC-2 has been postulated to contribute to cell volume control, we also examined regulatory volume decrease following cell swelling. However, parotid acinar cells from *Clcn2*$^{-/-}$ mice recovered volume with similar efficiency to wild-type littermates. These data demonstrate that ClC-2 is the hyperpolarization-activated Cl^- channel in salivary acinar cells but is not essential for maximum chloride flux during stimulated secretion of saliva or acinar cell volume regulation.

Molecular and functional studies have lead to the proposal that the inwardly rectifying Cl^- channel in most, if not all, mammalian cells is ClC-2. Indeed, a null mutation in the *Clcn2* gene resulted in the loss of hyperpolarization-activated anion currents in Leydig and Sertoli cells (1). Inwardly rectifying Cl^- currents have qualitatively similar properties in numerous tissues, nevertheless, unique activation kinetics are often observed in different cell types and in heterologous ClC-2 expression systems. For example, under identical experimental conditions, the chloride current generated by recombinant rat ClC-2 in HEK293 cells activates with a faster time course than the current in rat salivary acinar cells (2). Moreover, cAMP is an important regulator of recombinant human ClC-2 channel activity (3) and of hyperpolarization-activated Cl^- currents in both choroid plexus (4) and human T84 colon cells (5); in contrast, cAMP sensitivity is not seen in salivary acinar cells (6). One interpretation of these contrary results is differential expression of a regulatory subunit that modulates channel kinetics. Alternatively, splice variants of ClC-2 may alter the activation properties of this channel (7, 8). However, analysis of the currents in choroid plexus epithelial cells from ClC-2 knockout animals failed to reveal a loss of the hyperpolarization-activated Cl^- conductance (9). These later results demonstrate that another novel gene encodes the inwardly rectifying Cl^- current present in choroid plexus cells and raises the possibility that the hyperpolarization-activated Cl^- channel in salivary gland cells and other cell types is not ClC-2.

The physiological importance of some epithelial chloride channels has been revealed by gene mutation-inducing diseases such as cystic fibrosis (10), Bartter's syndrome (11), and nephrogenic diabetes insipidus (12). In mice lacking ClC-2, degeneration of the retina and testis occurs, indicating that this chloride channel is required for the survival of cells that depend on epithelia forming blood-organ barriers (1). It is unclear whether this barrier function is related to the regulation of ClC-2 activity by extracellular pH (13, 14) or cell swelling (15). The apical location of the ClC-2 channel in rat small intestine, renal, and airway epithelia further suggests that ClC-2 plays a role in regulating fluid and electrolyte movement in these tissues (16, 17). Indeed, antisense ClC-2 cDNA reduced native chloride current in the human intestinal cell line Caco-2 and significantly reduced Cl^--dependent secretion (16).

Genetic analysis has provided important and sometimes surprising insights into the function of several chloride channels. Nevertheless, a clear understanding of the physiological significance of ClC-2 and other chloride channels in most epithelia remains to be determined. Functional analysis is complicated in native epithelial cells, because multiple types of chloride channels are typically present. Salivary gland acinar cells are no exception, expressing at least five distinct chloride conductances (18, 19). The first of these to be characterized (20) is activated by an increase in intracellular free $[Ca^{2+}]_i$ (21). It is likely that the Ca^{2+}-dependent Cl^- channel is targeted to the apical membrane in parotid acinar cells as has been shown in pancreatic acinar cells (22). Because salivation is Ca^{2+}-depend-

* This work was supported in part by National Institutes of Health Grants DE09692 and DE13539 (to J. E. M.) and DK50594 (to G. E. S.). The costs of publication of this article were defrayed in part by the payment of page charges. This article must therefore be hereby marked "*advertisement*" in accordance with 18 U.S.C. Section 1734 solely to indicate this fact.

‡‡ To whom correspondence should be addressed: Center for Oral Biology, Aab Institute of Biomedical Sciences, University of Rochester Medical Center, Box 611, 601 Elmwood Ave., Rochester, NY 14642. Tel.: 585-275-3444; Fax: 585-506-0190; E-mail: james_melvin@urmc.rochester.edu.

ent (23–25), the Ca^{2+}-gated Cl^- channel has been predicted to be the primary Cl^- channel activated during stimulated secretion. Additional Cl^- channels found in salivary gland cells include those that are volume-sensitive (26), cAMP-dependent (18), hyperpolarization-activated (2, 19), and channels with properties like ClC-0 (18). The complexity created by the expression of multiple chloride channels in acinar cells indicates that gene knockout model systems will likely be required to unequivocally assign function to an individual channel.

Therefore, we disrupted the *Clcn2* gene to: 1) elucidate the molecular nature of the inwardly rectifying Cl^- current in salivary acinar cells; 2) determine the role of ClC-2 in saliva secretion; and 3) examine whether ClC-2 is critical for cell volume regulation. Patch-clamp analysis of chloride currents in salivary gland acinar cells demonstrated the loss of inwardly rectifying current in *Clcn2*$^{-/-}$ mice. In contrast, no changes were observed in the calcium- or volume-activated chloride conductances. Despite suggestions that ClC-2 may be involved in volume regulation, acinar cells from *Clcn2*$^{-/-}$ mice recovered cell volume following swelling by hypotonic shock as well as those from wild-type littermates. Furthermore, we show that the flow-rate of saliva secreted during *in vivo* stimulation, as well as the protein and electrolyte concentrations of the saliva, were comparable in wild-type and *Clcn2*$^{-/-}$ mice. These data unequivocally identity *Clcn2* as the gene that encodes for the inwardly rectifying Cl^- channel in salivary acinar cells and demonstrate that the Cl^- currents required for stimulated secretion of saliva are mediated by other channels such as the Ca^{2+}- and/or volume-activated Cl^- channels.

EXPERIMENTAL PROCEDURES

Generation of the Clcn2$^{-/-}$ *Mouse Strain*—A clone isolated from a 129/SVJ mouse genomic lambda library was used to construct a targeting vector with a neomycin-resistance (neo) gene as a positive selection marker and thymidine kinase gene as a negative selection marker. A 3.07-kb high fidelity PCR product obtained from a sub-cloned *Sst*I fragment from the *Clcn2* gene was inserted 3′ of the neo cassette, and a 2.3-kb *Eco*RI-*Bam*HI fragment was inserted 5′ of the neo cassette (see Fig. 1*A*). The neo cassette was designed to replace 1 kb of promoter and ~500 nucleotides of 5′-UTR[1] as well as exon 1 and most of exon 2 of the *Clcn2* gene. However, after blunt-end cloning the 5′-fragment, a clone containing the wrong orientation of the 5′-arm was mistakenly identified and subsequently linearized and electroporated into KG ES cells. Southern blotting of *Eco*RI-digested genomic DNA from targeted ES cell clones using a 1.3-kb outside probe (3′ of the sequence used to create the targeting vector, as indicated in Fig. 1*A*) led to the identification of a recombinant clonal isolate exhibiting the predicted 11- to 7-kb shift in size (Fig. 1*C*). Further characterization of this clone indicated that homologous recombination had taken place between the 3′-arm of the targeting vector and the genomic DNA, as well as between an unidentified segment of the 5′-arm of the targeting vector and a region slightly downstream of the 3′-end of the genomic copy of the 5′-arm (possibly due to the presence of long stretches of repetitive sequence in this area). Although this clone did not delete the promoter of the *Clcn2* gene, the replacement of most of exons 1 and 2 with PGKneo was expected to and did, in fact, result in the loss of both the ClC-2 transcript and protein in the final homozygous animal, as determined by RT-PCR and Western analysis (Fig. 1*D*). The generation of the anti-ClC2 antibody has been described previously (27) and is a kind gift of C. Bear (The Hospital for Sick Children, Toronto). Amino acids 16–35 of rat ClC-2 contain the target sequence to which the antibody was raised.

The targeted ES cell clone was injected into C57BL/6 blastocytes to generate chimeras that were backcrossed against the C57BL/6 strain. Germline transmission was assessed by Southern blotting, and heterozygous offspring were crossed to create the F2 animals used in the present study. In all cases, littermates were paired for each set of experiments. The general phenotype of our *Clcn2*$^{-/-}$ strain was essentially indistinguishable from that reported recently by the Jentsch laboratory (1). For histological examination, adult *Clcn2*$^{+/+}$ and *Clcn2*$^{-/-}$ age- and sex-matched littermates (7–8 weeks of age) were anesthetized with 300 mg of chloral hydrate/kg of body weight (intraperitoneally) and the tissues were fixed by perfusion with 10% neutral buffered formalin, sectioned at 5 μm, and stained with hematoxylin and eosin.

Electrophysiology—Whole cell currents were recorded at room temperature from freshly isolated single parotid acinar cells using the patch clamp technique (28). An Axopatch 200 B amplifier (Axon Instruments Corp., Foster City, CA) was used to voltage clamp and record the resulting chloride currents. Voltage clamp protocols to activate channels were generated by pClamp 8 software (Axon Instruments Corp.). Chloride currents were filtered at 1 kHz using a low pass Bessel filter and digitized at 2 kHz. A glass pipette had a 2- to 4-MΩ resistance when filled with the internal solutions. To record hyperpolarization-activated chloride currents, cells were dialyzed with an internal solution containing (millimolar): TEA-Cl 140, EGTA 20, HEPES 20, pH 7.3 with TEA-OH. Calcium-dependent chloride channel currents were recorded from cells dialyzed with an internal solution containing (millimolar): NMDG-glutamate 80, NMDG-EGTA 50, $CaCl_2$ 30, HEPES 20, pH 7.3 with NMDG. The free calcium concentration of this solution was estimated to be 250 nM (WinMax 2, Stanford CA). Cells were bathed in an external hypertonic solution containing (millimolar): TEA-Cl 140, $CaCl_2$ 0.5, D-mannitol 100, HEPES 20, pH 7.3 with TEA-OH; volume-sensitive currents were activated by diluting this solution 20% with water and using the same internal solution as described above for recording hyperpolarization-activated chloride currents. Square pulses of 5 or 3 s were delivered every 7 s from a holding potential of 0 (hyperpolarization-activated and volume-sensitive currents) or −50 mV (calcium-dependent currents). Membrane potential was changed between −120 to +120 mV in 20-mV steps, and the resulting currents were recorded after 10 (hyperpolarization-activated) and 5 (volume-sensitive and calcium-dependent currents) min of dialysis. Junction potentials (4.5 mV) and leak currents were not corrected. Current-voltage relationships were constructed by plotting the absolute magnitude of the currents at the end of the pulse against the membrane potential.

Acinar Cell Preparation—Parotid acinar cell clumps from adult (8–10 weeks old) *Clcn2*$^{+/+}$ and *Clcn2*$^{-/-}$ littermates were prepared by collagenase digestion as previously described (29). Briefly, mice were killed by exsanguination following exposure to CO_2 gas. The parotid glands were quickly removed, trimmed of connective tissues, and finely minced in 7.5 ml of collagenase digestion medium (Eagle's minimal essential medium, Biofluids, Inc., Rockville, MD) containing 0.04 mg/ml collagenase P and 1% BSA. The minced glands were incubated at 37 °C in a shaker with continuous agitation (100 cycles/min) and under gas (95%O_2 + 5%CO_2). After the first 20-min interval the minced glands were dispersed by gentle pipetting (10 times) and centrifuged (210 × *g* for 15 s). The supernatant was discarded, and the pellet was resuspended in 7.5 ml of collagenase digestion medium for an additional 40 min with pipetting at 20-min intervals. The cells were then rinsed and harvested by centrifugation.

Single cell preparations for electrophysiology utilized an initial 10-min digestion of the minced parotid tissue in 12.5 ml of trypsin digestion media (minimal essential medium, Spinner modification (SMEM), Biofluids, Inc.) containing 0.01% trypsin, 0.5 mM EDTA, and 1% BSA under 95%O_2 + 5%CO_2 gassing and while shaking (60 cycles/min). The cells were pelleted at 210 × *g* for 15 s then washed with 10 ml of trypsin inhibitor solution (SMEM containing 0.2% trypsin inhibitor and 1% BSA). The cells were spun again and incubated in collagenase digestion solution as described above. Single cells were rinsed with BSA-free basal medium Eagle, selected by filtration through 53-μm nylon mesh, and attached to circular 5-mm polylysine-coated glass coverslides in a 37 °C incubator containing 95%O_2 + 5%CO_2.

Cell Volume Determinations—Cell volume was estimated using a Nikon Diaphot 200 microscope interfaced with an Axon Imaging Workbench System (Novato, CA). The dispersed acinar cells were loaded with the fluoroprobe calcein by incubation for 15 min at room temperature with 100% O_2 in 2 μM calcein-AM (Molecular Probes, Eugene, OR). Dye-loaded cells were exposed to 490-nm light, and emitted fluorescence was measured at 530 nm. Changes in cell volume were monitored by measuring the fluorescence intensity of calcein within a delimited intracellular volume. Cell volume was expressed in arbitrary units as 1/normalized calcein fluorescence.

Hyposmotic Shock and the Subsequent Regulatory Volume Decrease—Calcein-loaded acinar cell clumps were equilibrated in an isotonic physiological solution containing (in millimolar): 135 NaCl, 5.4

[1] The abbreviations used are: UTR, untranslated repeat; RT-PCR, reverse transcription-PCR; CFTR, cystic fibrosis transmembrane conductance regulator; BSA, bovine serum albumin; SMEM, Spinner-modified minimal essential medium, RVD, regulatory volume decrease; NMDG, *N*-methyl-D-glucamine; TEA, tetraethylammonium.

KCl, 0.4 KH_2PO_4, 0.33 NaH_2PO_4, 20 Hepes, 10 glucose, 0.8 $MgSO_4$, and 1.2 $CaCl_2$, pH 7.4. Hypotonic challenge was induced by switching the perfusate to the above solution after diluting by 30% with water. Cell volume change was measured as described above. Regulatory volume decrease (RVD) was followed over the course of ~300 s while the cells remained in the hypotonic solution, and the rate of volume recovery was calculated by determining the slope of the best-fit line following the switch to hypotonic media and maximum cell swelling. Some experiments used clotrimazole (Sigma Chemical Co.) at a final concentration of 1 μM present in all of the solutions, and others used zinc at a final concentration of 50 μM.

Stimulated Flow Rates and Saliva Composition—Adult littermates *Clcn2*$^{+/+}$ and *Clcn2*$^{-/-}$ (7–8 weeks of age) were anesthetized with 300 mg of chloral hydrate/kg of body weight (intraperitoneally) and then stimulated with 10 mg of pilocarpine-HCl/kg of body weight (intraperitoneally). Whole saliva, primarily representing a combination of parotid and submandibular secretions, with a very minor component from sublingual and minor salivary, nasal, and tracheal glands, was collected from the lower cheek pouch by a suction device at intervals of 5, 10, and 15 min. The protein concentration of saliva was determined using the Bradford method. Total sodium and potassium contents in saliva samples were determined by atomic absorption using a PerkinElmer Life Sciences 3030 spectrophotometer. Saliva osmolality was measured using a Wescor 5500 vapor pressure osmometer, and chloride activity was determined using an Orion EA 940 expandable ion analyzer.

RESULTS

Generation of a Mouse Strain Lacking ClC-2—A lambda genomic DNA library derived from 129/SVJ mice was screened using a probe specific for the *Clcn2* gene. Genomic fragments from the resulting lambda clone were used to flank a positive (PGKneo) selection cassette in a vector designed to target the *Clcn2* gene for disruption (Fig. 1*A*). The construct was intended to replace a genomic segment that includes a portion of the *Clcn2* promoter and 5′-UTR, as well as all of exon 1 and most of exon 2, with PGKneo. This strategy was expected to result in the inability to initiate transcription from the defunct *Clcn2* promoter in the transgenic strain, causing an absence of functional protein, thereby avoiding the possibility of a dominant negative effect caused by expression of a truncated protein. During the gene-targeting procedure, a construct with the upstream arm in the wrong orientation was mistakenly utilized. Electroporation of this construct into embryonic stem cells resulted in a single targeted cell line (out of ~900 neomycin-resistant clones; Fig. 1*C*) resulting from a hybrid homologous recombination/insertion event, as described below. After the mistake was recognized we learned that the promoter of another gene, encoding the RPB-17 protein, overlaps that of *Clcn2* in rat (30), as well as in mouse.[2] Because the correct construct would disrupt both genes, we proceeded to analyze the embryonic stem cell clone that we had identified.

Analysis using both inside and outside probes as well as genomic PCR (data not shown) demonstrated that homologous recombination occurred between the 3′-arm of the targeting vector and the *Clcn2* gene. This was followed by a non-homologous insertion event in the upstream (backwardly oriented) arm (Fig. 1*B*). The junction between the genomic and vector DNA was not mapped at the single nucleotide level due to a stretch of over 1500 nucleotides of up to 85% GC content, which precluded genomic PCR across that region. The final homozygous knockout strain was shown to lack ClC-2 protein by Western analysis (Fig. 1*D*). In addition, RT-PCR with primers to the 5′- and 3′-ends of the transcript confirmed that ClC-2 message was not present in the knockout strain, whereas Northern analysis indicated that the RPB-17 mRNA, whose promoter overlaps that of *Clcn2*, but in the antisense orientation, was present at normal levels in the *Clcn2*$^{-/-}$ animal (data not shown).

[2] K. Nehrke, unpublished observations.

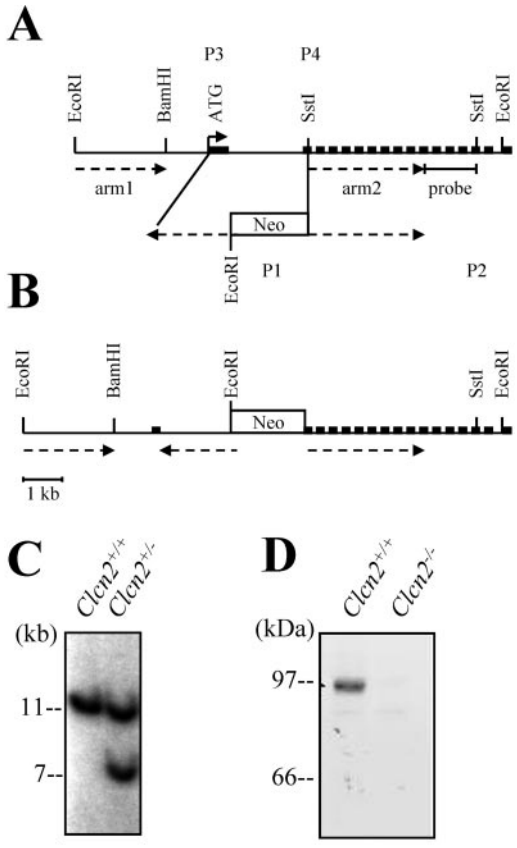

FIG. 1. **Clcn2 gene targeting.** *A*, schematic of the design used to create the *Clcn2* gene targeting construct. The genomic DNA is represented by the *upper drawing*, whereas the targeting construct is represented by the *lower drawing*. Approximate sites where replacement of the genomic DNA with the targeting construct occurred are indicated by *lines* joining the *upper* and *lower drawings*. Homologous arms 1 and 2 correspond to the promoter region of *Clcn2* and from exon 2 through exon 11 of the coding region, respectively, and are indicated by *dashed arrows*. An outside probe, denoted in the schematic, was used to identify recombinant clones based upon Southern analysis of genomic *Eco*RI digests. Primers 1 and 2 (*P1* and *P2*) were used in genomic PCR of the targeted strain, and sequencing of the PCR product indicated that recombination had occurred in the 3′-arm as predicted. Primers 3 and 4 (*P3* and *P4*) failed to produce an RT-PCR product from the targeted strain, as did a combination of primer 2 (*P2*) and a primer antisense to primer 4 (*P4*), confirming the lack of ClC-2 message. *B*, schematic of the final targeted clone. An apparent recombination/insertion event resulted in the inverted duplication of arm 1, as indicated by the *dashed arrows* facing each other. The junction between the inserted vector DNA and the genomic DNA was not mapped at the nucleotide level, due to a stretch of nearly 85% GC-rich DNA in the region that precluded genomic PCR. *C*, Southern analysis of *Eco*RI-digested genomic DNA from a targeted ES cell line, using the outside probe indicated above. *D*, Western analysis of ClC-2 protein from brain homogenates prepared from *Clcn2*$^{+/+}$ and $^{-/-}$ strains.

Retinal and Testicular Degeneration in ClC-2-deficient Mice—The phenotype of the *Clcn2*$^{-/-}$ strain generated in our laboratory is comparable to that reported recently (1). The mice appeared generally healthy and displayed normal behavior and body weight, but histological examination of semi-thin sections revealed abnormalities of the eye and testis. Unlike the wild-type eye (Fig. 2*A*), the knockout exhibited post-natal degeneration of the retina, reflected by a gradual loss of photoreceptor cells and the outer nuclear layer, which was not present or remained as only a few cells adjacent to the inner nuclear layer (Fig. 2, *B* and *C*). Maturation of the testes was normal in wild-type mice (Fig. 3*A*) but was impaired in the knockout (Fig. 3*B*). In *Clcn2*$^{-/-}$ mice at the age of sexual maturity, the germ cell layers were missing, and no mature spermatozoa were present; in addition, there was hyperplasia of the Leydig cells

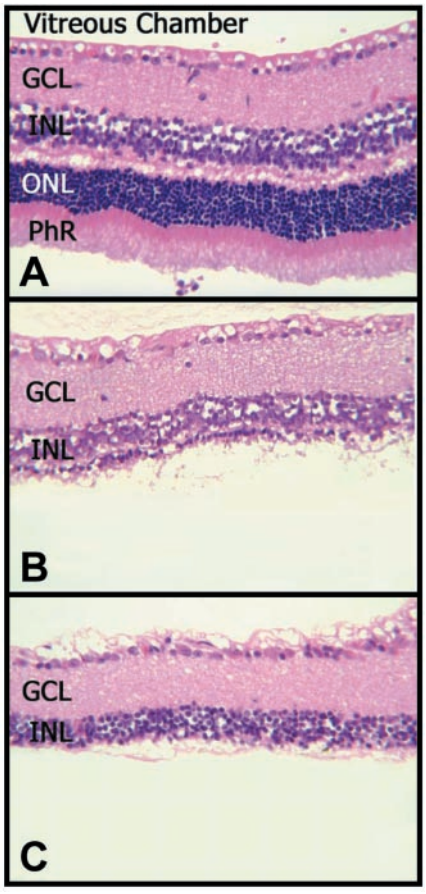

FIG. 2. **Histology of the retina.** *A*, retina from a *Clcn2*$^{+/+}$ female, with normal architecture, including inner nuclear layer (*INL*), outer nuclear layer (*ONL*), ganglion cell layer (*GCL*), and photoreceptors (*PhR*). *B*, retina from a *Clcn2*$^{-/-}$ female, with decreased outer nuclear layer, and a single row of photoreceptor nuclei remaining adjacent to the inner nuclear layer. *C*, retina from a *Clcn2*$^{-/-}$ male, which has lost all of the photoreceptor nuclei, leaving only the inner nuclear layer.

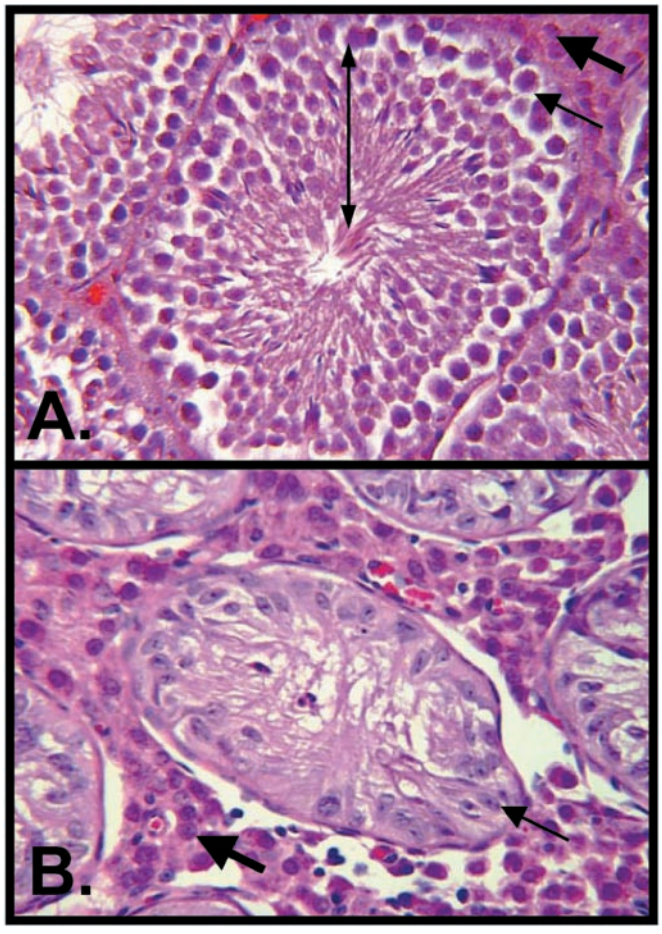

FIG. 3. **Histology of the testis.** 5-μm sections of testis from a *Clcn2*$^{+/+}$ male (*A*) and *Clcn2*$^{-/-}$ male (*B*) obtained 10 weeks after birth. The normal testicular architecture found in the $^{+/+}$ mice is compromised in the *Clcn2*$^{-/-}$ animal, with missing germ cell layers (*double-headed arrow* in the +/+ control), abnormal Sertoli cells (*small arrows*) and a relative hyperplasia of the Leydig cells (*large arrows*).

and abnormal Sertoli cells were prominent and widespread (Fig. 3*B*).

Characterization of Chloride Currents from Parotid Acinar Cells—The homozygous knockout strain was used to assess the molecular nature of the inwardly rectifying Cl^- current and to determine the role of ClC-2 in saliva gland function and fluid secretion from salivary acinar cells. The production of saliva is initiated by an increase in intracellular Ca^{2+} that opens Ca^{2+}-dependent chloride channels on the apical membranes of the acinar cells. Anion fluxes in parotid acinar cells are mediated by at least five distinct chloride currents, namely, volume-sensitive, calcium-dependent, cAMP-activated, ClC-0-like, and hyperpolarization-activated channels (18, 19). RT-PCR has demonstrated the presence of ClC-2 in parotid acini, and the characteristics of the hyperpolarization-activated chloride current in this cell type are quantitatively similar to that of the cloned ClC-2 channel (2). To unambiguously determine the molecular identity of the channel mediating this current, we performed patch clamp analysis on single parotid acinar cells isolated from wild-type and *Clcn2*$^{-/-}$ mice.

The chloride currents recorded from wild-type parotid acinar cells using the whole cell configuration (Fig. 4, *upper left trace*) displayed inward rectification and time dependence, as has been observed previously (2, 19). To clearly monitor the hyperpolarization-activated chloride currents, it was necessary to eliminate the Ca^{2+}-dependent and the volume-sensitive currents. This was accomplished using an internal pipette solution containing the calcium chelator EGTA and a hypertonic bath solution (see "Experimental Procedures"). Relative to acini from wild-type mice, currents for the acini of *Clcn2*$^{-/-}$ mice decreased more than 10-fold in magnitude at the most negative potentials and exhibited no rectification (Fig. 4, *upper right trace*). The *lower panels* show the current-voltage (IV) relations of chloride currents for parotid acinar cells derived from multiple *Clcn2*$^{+/+}$ (left, $n = 6$) and *Clcn2*$^{-/-}$ (right, $n = 8$) mice. A similar analysis of heterozygous *Clcn2*$^{+/-}$ mice revealed similar hyperpolarization-activated currents as present in wild-type acinar cells, suggesting that there is no dominant negative effect (data not shown). These results confirm that the ClC-2 channel is, in fact, responsible for the hyperpolarization-activated Cl^- current in parotid acinar cells.

Because the opening of the Ca^{2+}-activated Cl^- channel on the apical cell membrane is thought to be the primary means through which chloride exits the cell following stimulation, we examined Ca^{2+}-dependent chloride currents in the *Clcn2*$^{-/-}$ mice as well. Although it is unlikely that ClC-2 contributes to the Ca^{2+}-activated chloride current directly, oftentimes gene ablations lead to compensatory mechanisms in overlapping or redundant processes (31, 32). Fig. 5 (*upper panels*) shows whole cell Ca^{2+}-dependent Cl^- current obtained from wild-type (*left*) and *Clcn2*$^{-/-}$ (*right*) mice; the *lower panels* show the corresponding average current-voltage relationships. Thus, the Ca^{2+}-dependent Cl^- currents from the *Clcn2*$^{-/-}$ mice resembled those from *Clcn2*$^{+/+}$ mice, although with greater variability in magnitude.

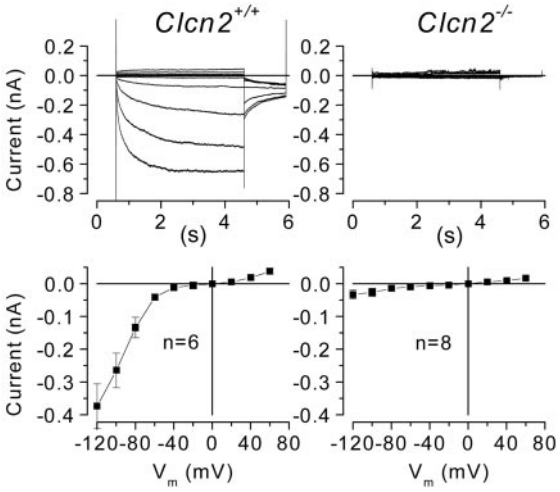

FIG. 4. **Chloride currents in *Clcn2*$^{+/+}$ and *Clcn2*$^{-/-}$ mice.** *Upper panels*, whole cell chloride currents recorded from single acinar cells isolated from wild-type *Clcn2*$^{+/+}$ (*left*) and *Clcn2*$^{-/-}$ (*right*) mice. *Lower panels*, current voltage relationships from *Clcn2*$^{+/+}$ (*left*; $n = 6$) and *Clcn2*$^{-/-}$ (*right*; $n = 8$) mice, respectively. The internal solution contained (millimolar): TEA-Cl 140, EGTA 20, HEPES 20, pH 7.3, with TEA-OH, whereas the external solution contained (millimolar): TEA-Cl 140, $CaCl_2$ 0.5, D-mannitol 100, HEPES 20, pH 7.3, with TEA-OH.

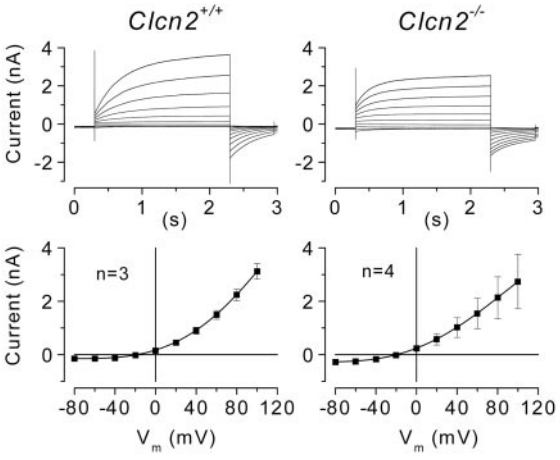

FIG. 5. **Calcium-dependent chloride currents in *Clcn2*$^{+/+}$ and *Clcn2*$^{-/-}$ mice.** The *upper panels* display calcium-dependent currents recorded from single parotid acinar cells isolated from *Clcn2*$^{+/+}$ (*left*) and *Clcn2* $^{-/-}$ (*right*) mice, respectively. The *lower panels* are the respective corresponding averaged current voltage relationships (*Clcn2*$^{+/+}$, $n = 3$; *Clcn2* $^{-/-}$, $n = 4$). The internal solution contained (millimolar): NMDG-glutamate 80, NMDG-EGTA 50, $CaCl_2$ 30, HEPES 20, pH 7.3, with NMDG, whereas the external solution contained (millimolar): TEA-Cl 140, $CaCl_2$ 0.5, D-mannitol 100, HEPES 20, pH 7.3, with TEA-OH.

ClC-2 Does Not Function in Regulatory Volume Decrease in Parotid Acinar Cells—Mammalian cells undergo a regulatory volume decrease (RVD) upon exposure to a hypotonic medium. This process allows the efflux of electrolytes, which are then followed osmotically by water, resulting in cell shrinkage to a normal resting volume. ClC-2 has been shown to be up-regulated by cell swelling and may play a role in RVD (15, 33–35), although some evidence exists that ClC-2 can be inhibited by hypotonicity as well, in the presence of protein phosphatase inhibitors (36). Fig. 6 shows that under hypertonic conditions ClC-2 Cl^- currents were present in acinar cells from wild-type (*upper left*) but not *Clcn2*$^{-/-}$ (*upper right*) mice. In contrast, upon exposing the same cells to a hypotonic solution, large, outwardly rectifying chloride currents similar to those previously reported (26) were recorded in acinar cells from both genotypes (Fig. 6). The currents activated under hypotonic

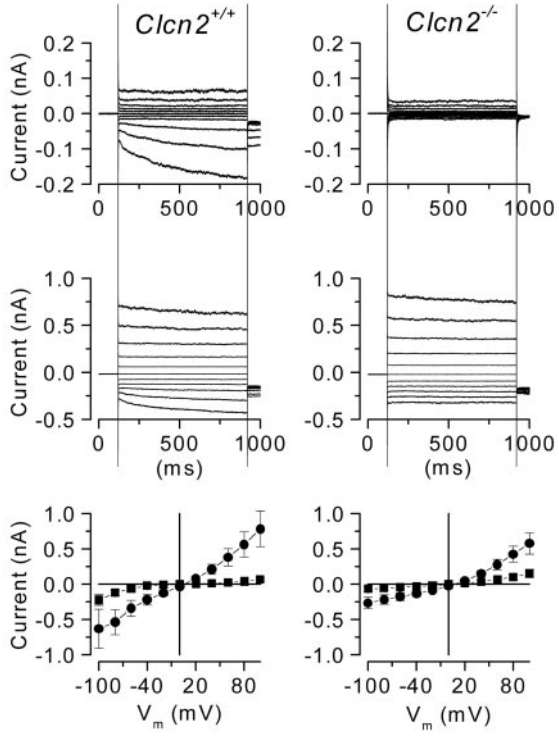

FIG. 6. **Volume-stimulated chloride currents in *Clcn2*$^{+/+}$ and *Clcn2*$^{-/-}$ mice.** The *left* and *right columns* display data obtained from *Clcn2*$^{+/+}$ and *Clcn2*$^{-/-}$ mice, respectively. *Upper panel*, control currents obtained from −100 to + 100 mV after 6-min dialysis. Note that the scale is reduced in comparison to the *middle panel* to observe the currents more clearly. *Middle panel*, chloride currents obtained from the same cells depicted in the *upper row* after 4 min in a 20% hypotonic medium. *Lower panel*, average current-voltage relationships obtained from cells under control conditions (*squares*) and after 4 min in a hypotonic solution (*circles*). (*Clcn2*$^{+/+}$, $n = 4$; *Clcn2*$^{-/-}$, $n = 3$). The internal solution contained (millimolar): TEA-Cl 140, EGTA 20, HEPES 20, pH 7.3, with TEA-OH, whereas the external solution contained (millimolar): TEA-Cl 140, $CaCl_2$ 0.5, D-mannitol 100, HEPES 20, pH 7.3, with TEA-OH, which was diluted by 20% with water to activate the currents.

conditions did not resemble those of ClC-2, nor were they altered in *Clcn2*$^{-/-}$ acinar cells (Fig. 6, *middle right trace*). Also the magnitude of the time-dependent current due to ClC-2 activation at −100 mV in wild-type acinar cells was not altered by cell swelling. The IV curves derived from multiple *Clcn2*$^{+/+}$ and *Clcn2*$^{-/-}$ mice indicated that there was no significant change in the swelling-activated chloride currents (Fig. 6, *lower panels*).

To ascertain whether ClC-2 contributes functionally to volume regulation in parotid acinar cells, cell volume changes were monitored following swelling in hypotonic solution (Fig. 7*A*) and the initial rates of RVD were determined. Parotid acini from *Clcn2*$^{-/-}$ mice underwent RVD following swelling at a similar initial rate as their wild-type littermates (Fig. 7*B*). In addition, the divalent cation Zn^{2+} is known to inhibit ClC-2 chloride currents expressed in *Xenopus* oocytes (37) and mouse parotid acinar cells (13), but had no effect on the initial rate of RVD in wild-type parotid acinar cells (Fig. 7*B*). On the other hand, clotrimazole, a relatively specific inhibitor of IK1 Ca^{2+}-activated K^+ channels (38), reduced the initial rate of RVD by 50% (Fig. 7*B*). Together, these data suggest that ClC-2 is not a major regulator of cell volume homeostasis in parotid acinar cells.

Loss of Inwardly Rectifying ClC-2 Chloride Channels Does Not Change the Composition or Flow Rate of Whole Saliva—The functional consequences of disrupting expression of the

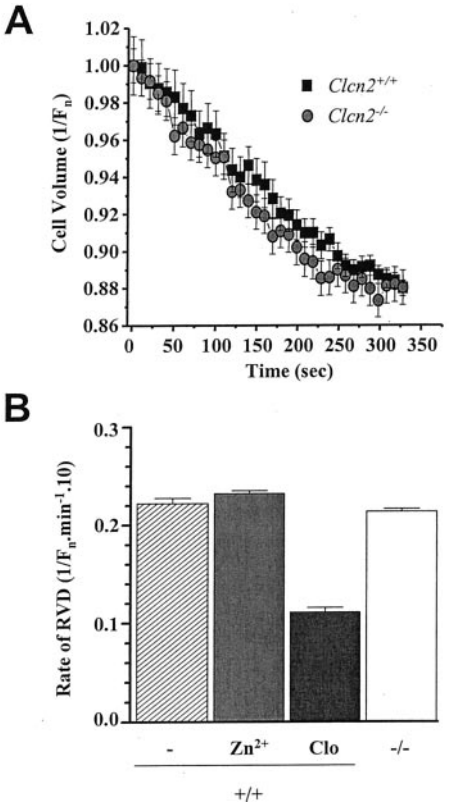

FIG. 7. **Regulatory volume decrease in parotid acinar cells from mice lacking ClC-2 expression.** The role of ClC-2 in the RVD response was examined in parotid acini loaded with calcein as described under "Experimental Procedures." *A*, parotid acini isolated from $Clcn2^{+/+}$ (*black squares*) and $Clcn2^{-/-}$ (*gray circles*) mice were perfused in an isosmotic solution, and then swelling was induced by switching the perfusate to a hypotonic medium (30% dilution with water). Changes in cell volume were expressed as 1/calcein F_n, and the initial rate of RVD was calculated ($Clcn2^{+/+}$, $n = 7$ and $Clcn2^{-/-}$, $n = 11$; representing four separate acinar cell preparations). *B*, the initial rate of RVD was calculated for $Clcn2^{+/+}$ ($n = 21$) and $Clcn2^{-/-}$ ($n = 23$) acini and for wild-type acini treated with either 50 μM zinc ($n = 19$) to inhibit ClC-2 channels or with 1 μM clotrimazole ($n = 20$) to inhibit the Ca^{2+}-activated K^+ channel mIK1.

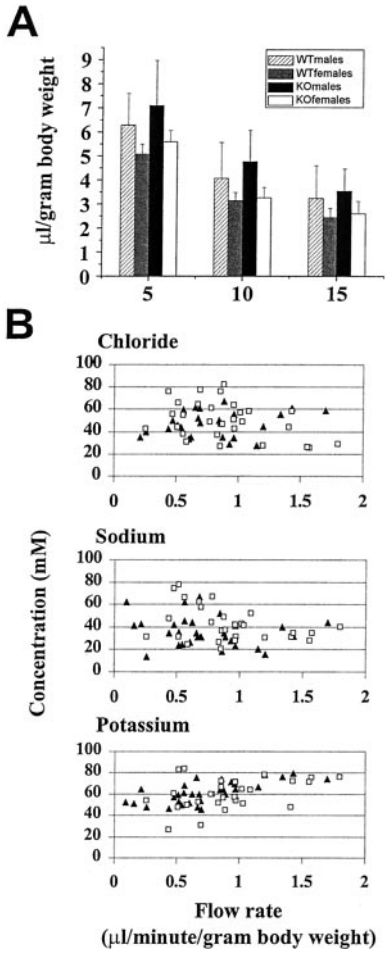

FIG. 8. **Saliva flow rates and flow rate dependence of salivary electrolyte concentrations in wild-type and ClC-2 knockout mice.** *A*, whole saliva was collected at 5-min intervals over a 15-min period from mice stimulated to secrete with the cholinergic agonist pilocarpine (10 mg/kg intraperitoneally). The volume of saliva collected was normalized to the body weight of the mice. Standard deviations are presented for each of the four groups analyzed: $Clcn2^{+/+}$ and $Clcn2^{-/-}$ males ($n = 11$ each) and $Clcn2^{+/+}$ and $Clcn2^{-/-}$ females ($n = 5$ each). More males than females were analyzed due to higher variability among male animals. *B*, individual salivary flow rates were calculated for each 5-min sample taken from every animal as indicated above then compared with the concentrations of the electrolytes chloride, sodium, and potassium in the mature saliva (▲, $Clcn2^{+/+}$; □, $Clcn2^{-/-}$).

inwardly rectifying ClC-2 Cl^- channel in salivary glands was first examined by determining the amount of saliva secreted following stimulation with the cholinergic agonist pilocarpine. Whole saliva, an indicator of overall salivary gland function (38), was collected from age- and sex-matched littermates at 5-min intervals over a 15-min period. The saliva collected here primarily represents contributions from the parotid and submandibular salivary glands, as well as a smaller component from sublingual and minor salivary glands, and nasal secretions. ClC-2 is present in both the parotid and submandibular glands (2, 18). Changes in the ability of these glands to secrete fluid are reflected in the accumulation of whole saliva in the oral cavity. However, a comparison between wild-type and $Clcn2^{-/-}$ mice failed to reveal significant differences for either the average flow rates at any point during the collection period (Fig. 8*A*) or the total volume of saliva secreted (Table I). Over the course of the 15-min collection period, male $Clcn2^{+/+}$ and $Clcn2^{-/-}$ mice secreted 13.6 ± 3.4 and 15.4 ± 3.6 μl of saliva per gram of body weight, respectively, while female wild-type and $Clcn2^{-/-}$ mice secreted 10.1 ± 1.0 and 11.4 ± 2.6 μl per gram of body weight, respectively.

As previously observed (39), the average flow rates became slower as time progressed (Fig. 8*A*), but the concentrations of the electrolytes sodium, chloride, and potassium were qualitatively similar at both higher and lower flow rates in both genotypes (Fig. 8*B*). This point is important as it is during transit of the primary secretions through the water-impermeable ductal network that electrolytes (primarily Na^+ and Cl^-) are reabsorbed, leading to a NaCl-poor, hypotonic mature secretion, and ClC-2-like Cl^- currents have been described in salivary gland duct cells (40). We note here that we are using pilocarpine, which is a mixed cholinergic agonist that activates both sympathetic and parasympathetic components, via nicotinic and muscarinic receptors, respectively, to stimulate salivation, and that salivary gland duct cells are also responsive to beta-adrenergic agonists; thus, although the data strongly suggest that ClC-2 is not involved in electrolyte conservation in salivary glands under these conditions, the data do not completely rule out a role for ClC-2 in duct function under all conditions. Finally, we demonstrated that the total amount of protein present in the saliva was not significantly different in knockout mice compared with their sex-matched wild-type littermates and showed that the weights of the salivary glands were similar in both wild-type and $Clcn2^{-/-}$ mice (Table I). Although our results suggest that ClC-2 is involved in neither secretion from salivary acinar cells following cholinergic stim-

TABLE I

Volume and composition of saliva from Clcn2$^{+/+}$ and Clcn2$^{-/-}$ mice

Whole saliva was collected following stimulation with the cholinergic agonist pilocarpine. The total volumes of saliva secreted over a 15-min period are given for eleven male and five female age- and sex-matched pairs (standard deviations are given in parenthesis). A greater number of male replicate pairs were examined due to a greater deviation in the total volume secreted from the males. The total protein contents of the secretions and the corresponding osmolarities were determined, as well, and the major salivary glands were excised and weighed immediately following saliva collection. For these determination, an equal number of replicate pairs were used for both female and male mice.

	Male		Female	
	Clcn2$^{+/+}$	Clcn2$^{-/-}$	*Clcn2$^{+/+}$*	*Clcn2$^{-/-}$*
Saliva volume (μl/gram body weight/15 min), male $n = 11$; female, $n = 5$	13.6 (±3.4)	15.4 (±3.6)	10.1 (±1.0)	11.4 (±2.6)
Protein (mg/gram body weight/15 min), $n = 3$	0.51 (±0.23)	0.82 (±0.09)	0.81 (±0.13)	1.18 (±0.35)
Osmolarity (mosM), $n = 5$	195.5 (±12.5)	195.9 (±21.3)	187.3 (±22.3)	203.6 (±17.5)
Parotid weight (mg), $n = 4$	104.3 (±23.4)	93.4 (±21.7)	75.3 (±22.7)	84.9 (±20.8)
Submandibular weight (mg), $n = 4$	138.9 (±11.1)	133.7 (±4.0)	73.3 (±6.2)	80.8 (±12.1)
Sublingual weight (mg), $n = 4$	20.0 (±1.3)	20.3 (±1.3)	20.5 (±5.2)	21.4 (±6.7)

ulation nor electrolyte conservation in the salivary ductal network, it remains a possibility that unknown compensatory mechanisms are at work.

DISCUSSION

ClC-2 is a broadly expressed plasma membrane chloride channel that is active at negative membrane potentials (41). Although the function of other members of the ClC gene family have become clear following the identification of disease phenotypes associated with their mutation, the role of ClC-2 remains an enigma. The distribution of ClC-2 and its overlap with that of the cystic fibrosis transmembrane conductance regulator (CFTR), the CF gene product, suggests an important function for ClC-2 in maintaining chloride homeostasis as well as the potential to serve a compensatory role in alleviating the severity of the CF phenotype. ClC-2 has been shown to be present in the developing fetal lung (42, 43), as well as in the small intestinal epithelium (27), and contributes to chloride secretion from an intestinal cell line (16). However, mice deficient in ClC-2 displayed no gross phenotypic deficits in intestinal or lung function.

The focus of the present study was to test three hypotheses in mice deficient in the expression of ClC-2. 1) Is ClC-2 the hyperpolarization-activated Cl^- channel in salivary acinar cells? 2) Does ClC-2 contribute to saliva secretion? 3) Is ClC-2 involved in cell volume regulation? In agreement with a previous report (1), we found that the only apparent global phenotypic deficits associated with the lack of ClC-2 include postnatal degeneration of the retina, including loss of the outer nuclear layer, which results in blindness, and incomplete maturation of the seminiferous tubules and abnormal Sertoli cells in the testes, leading to azoospermatic males that are infertile. A common theme among these phenotypes is the dependence of the retina and seminiferous tubules on close cell-cell interactions, as noted by Bösl and colleagues (2001). Briefly, both affected organs are protected by a blood-organ barrier, and degeneration occurs in cells that depend upon the barrier-forming epithelium (for a more detailed discussion, see Ref. 1). Interestingly, a *Caenorhabditis elegans* homolog of ClC-2, termed CLH-3, has recently been characterized (44). Although CLH-3 can be activated by cell swelling, the physiological trigger for activation is the induction of oocyte meiotic maturation. In animals exhibiting a CLH-3 loss-of-function, the contractile activity of gonadal sheath cells is initiated prematurely. Thus, the function of this channel is to couple two processes that occur between adjacent cells. How this is accomplished is not known at the present time. However, in mice, ClC-2 has been localized to the tight junction complex between adjacent intestinal epithelial cells (27) and phenotypically, the *Clcn2$^{-/-}$* mice exhibit deficits in male germs cells and photoreceptor cells, both dependent upon close cell-cell interactions. It is possible that this member of the ClC family acts in barrier function and cell-cell communication, raising the question of whether these processes may be codependent or coupled in some fashion. Further study of exactly how the loss of ClC-2 leads to these phenotypes will undoubtedly shed light on its physiological role.

In contrast to the studies of choroid plexus epithelial cells by Speake *et al.* (9), we found that targeted disruption of the *Clcn2* gene resulted in loss of the inwardly rectifying Cl^- current in salivary acinar cells. Based upon its location in other polarized cell types, ClC-2 could act at the apical acinar cell surface to potentiate Cl^- efflux into the lumen of the gland during stimulation by acting in concert with other Cl^- channels. The Ca^{2+}-dependent Cl^- channel is targeted to the apical membrane, however, down-regulation of this channel is frequently observed (45, 46). This suggests that an additional Cl^- channel might also be activated in response to sustained stimulation, possibly by a non-Ca^{2+}-dependent mechanism. It is doubtful that the volume-sensitive Cl^- channel fills this role, because cell shrinkage, which occurs during stimulation (47), down-regulates this channel (26). Moreover, the cAMP-dependent channel, almost certainly encoded by the *Cftr* gene (18), is not significantly involved in salivation. Functionally, due to the strong hyperpolarization required to gate ClC-2, it is unclear whether ClC-2 would be very active under physiological conditions. In fact, we found that normal levels of secretion occur in the Clcn2$^{-/-}$ mice. Moreover, ClC-2 played little, if any, role in cell volume regulation in salivary acinar cells. Although our data suggest that ClC-2 is involved in neither fluid secretion nor cell volume regulation in salivary glands, we cannot exclude the possibility that ClC-2 may function in such roles in other epithelial tissues or that yet unknown compensatory mechanisms alleviate the loss of ClC-2 in the salivary cells.

The movement of the primary secretions through duct cells in salivary glands allows reabsorption of electrolytes, including chloride and sodium, and results in a hypotonic NaCl-poor final secretion. The molecular mechanism by which these electrolytes are reabsorbed is still not understood, but most likely involves the epithelial sodium channel (48–51), with chloride moving either paracellularly or through a chloride channel located on the apical membrane of the ducts. Normal levels of sodium, chloride, and potassium were found in the saliva of *Clcn2$^{-/-}$* mice; this, combined with the normal osmolarity of the saliva, suggests that ClC-2 is not a major pathway for regulating electrolyte reabsorption in salivary glands following cholinergic stimulation. However, duct cells are also responsive to beta-adrenergic stimulation and several types of Cl^- currents (52, 53), including ClC-2-like currents (40), have been previously described in these cells. Thus, other Cl^- channels such as CFTR could compensate for and reduce the phenotypic severity of ClC-2 loss under the appropriate conditions.

In summary, we have shown that ablation of the *Clcn2* gene

does not result in notable deficits in either the production or modification of saliva following stimulation with a cholinergic agonist in mice, despite the loss of inward-rectifying Cl^- current. Moreover, the phenotypic defects observed in the *Clcn2*$^{-/-}$ mice indicate that the ClC-2 chloride channel is involved in the continued viability of both retinal and testicular cells; this may reflect a role in cell-cell communication, as is the case with CLH-3, the *C. elegans* ClC-2 ortholog.

Acknowledgment—We thank Dr. Christine Bear for reagents and technical assistance in assessing the level of ClC-2 protein in the knockout strain.

REFERENCES

1. Bosl, M. R., Stein, V., Hubner, C., Zdebik, A. A., Jordt, S. E., Mukhopadhyay, A. K., Davidoff, M. S., Holstein, A. F., and Jentsch, T. J. (2001) *EMBO J.* **20,** 1289–1299
2. Park, K., Arreola, J., Begenisich, T., and Melvin, J. E. (1998) *J Membr. Biol.* **163,** 87–95
3. Tewari, K. P., Malinowska, D. H., Sherry, A. M., and Cuppoletti, J. (2000) *Am. J. Physiol.* **279,** C40–C50
4. Kibble, J. D., Trezise, A. E., and Brown, P. D. (1996) *J. Physiol.* **496,** 69–80
5. Fritsch, J., and Edelman, A. (1996) *J. Physiol.* **490,** 115–128
6. Park, K., Begenisich, T., and Melvin, J. E. (2001) *J. Membr. Biol.* **182,** 31–37
7. Chu, S., and Zeitlin, P. L. (1997) *Nucleic Acids Res.* **25,** 4153–4159
8. Cid, L. P., Niemeyer, M. I., Ramirez, A., and Sepulveda, F. V. (2000) *Am. J. Physiol.* **279,** C1198–C1210
9. Speake, T., Kajita, H., Smith, C. P., and Brown, P. D. (2002) *J. Physiol.* **539,** 385–390
10. Riordan, J. R., Rommens, J. M., Kerem, B., Alon, N., Rozmahel, R., Grzelczak, Z., Zielenski, J., Lok, S., Plavsic, N., and Chou, J. L., Drumm, M. L., Iannuzzi, M. C., Collins, F. S., and Tsui, L.-S. (1989) *Science* **245,** 1066–1073
11. Simon, D. B., Bindra, R. S., Mansfield, T. A., Nelson-Williams, C., Mendonca, E., Stone, R., Schurman, S., Nayir, A., Alpay, H., Bakkaloglu, A., Rodriguez-Soriano, J., Morales, J. M., Sanjad, S. A., Taylor, C. M., Pilz, D., Brem, A., Trachtman, H., Griswold, W., Richard, G. A., John, E., and Lifton, R. P. (1997) *Nat. Genet.* **17,** 171–178
12. Matsumura, Y., Uchida, S., Kondo, Y., Miyazaki, H., Ko, S. B., Hayama, A., Morimoto, T., Liu, W., Arisawa, M., Sasaki, S., and Marumo, F. (1999) *Nat. Genet.* **21,** 95–98
13. Arreola, J., Begenisich, T., and Melvin, J. E. (2002) *J. Physiol. (Lond.)* **541,** 103–112
14. Jordt, S. E., and Jentsch, T. J. (1997) *EMBO J.* **16,** 1582–1592
15. Gründer, S., Thiemann, A., Pusch, M., and Jentsch, T. J. (1992) *Nature* **360,** 759–762
16. Mohammad-Panah, R., Gyomorey, K., Rommens, J., Choudhury, M., Li, C., Wang, Y., and Bear, C. E. (2001) *J. Biol. Chem.* **276,** 8306–8313
17. Murray, C. B., Chu, S., and Zeitlin, P. L. (1996) *Am. J. Physiol.* **271,** L829–L837
18. Zeng, W., Lee, M. G., and Muallem, S. (1997) *J. Biol. Chem.* **272,** 32956–32965
19. Arreola, J., Park, K., Melvin, J. E., and Begenisich, T. (1996) *J. Physiol.* **490,** 351–362
20. Iwatsuki, N., Maruyama, Y., Matsumoto, O., and Nishiyama, A. (1985) *Jpn. J. Physiol.* **35,** 933–944
21. Arreola, J., Melvin, J. E., and Begenisich, T. (1996) *J. Gen. Physiol.* **108,** 35–47
22. Park, M. K., Lomax, R. B., Tepikin, A. V., and Petersen, O. H. (2001) *Proc. Natl. Acad. Sci. U. S. A.* **98,** 10948–10953
23. Melvin, J. E., Koek, L., and Zhang, G. H. (1991) *Am. J. Physiol.* **261,** G1043–G1050
24. Martinez, J. R., and Petersen, O. H. (1972) *Experientia* (*Basel*) **28,** 167–168
25. Douglas, W. W., and Poisner, A. M. (1963) *J. Physiol.* **165,** 528–541
26. Arreola, J., Melvin, J. E., and Begenisich, T. (1995) *J. Physiol.* **484,** 677–687
27. Gyomorey, K., Yeger, H., Ackerley, C., Garami, E., and Bear, C. E. (2000) *Am. J. Physiol.* **279,** C1787–C1794
28. Hamill, O. P., Marty, A., Neher, E., Sakmann, B., and Sigworth, F. J. (1981) *Pflugers Arch.* **391,** 85–100
29. Evans, R. L., Bell, S. M., Schultheis, P. J., Shull, G. E., and Melvin, J. E. (1999) *J. Biol. Chem.* **274,** 29025–29030
30. Chu, S., Blaisdell, C. J., Liu, M. Z., and Zeitlin, P. L. (1999) *Am. J. Physiol.* **276,** L614–L624
31. Schultheis, P. J., Clarke, L. L., Meneton, P., Miller, M. L., Soleimani, M., Gawenis, L. R., Riddle, T. M., Duffy, J. J., Doetschman, T., Wang, T., Giebisch, G., Aronson, P. S., Lorenz, J. N., and Shull, G. E. (1998) *Nat. Genet.* **19,** 282–285
32. Brooks, H. L., Sorensen, A. M., Terris, J., Schultheis, P. J., Lorenz, J. N., Shull, G. E., and Knepper, M. A. (2001) *J. Physiol.* **530,** 359–366
33. Furukawa, T., Ogura, T., Katayama, Y., and Hiraoka, M. (1998) *Am. J. Physiol.* **274,** C500–C512
34. Xiong, H., Li, C., Garami, E., Wang, Y., Ramjeesingh, M., Galley, K., and Bear, C. E. (1999) *J. Membr. Biol.* **167,** 215–221
35. Roman, R. M., Smith, R. L., Feranchak, A. P., Clayton, G. H., Doctor, R. B., and Fitz, J. G. (2001) *Am. J. Physiol.* **280,** G344–G353
36. Fritsch, J., and Edelman, A. (1997) *Am. J. Physiol.* **272,** C778–C786
37. Clark, S., Jordt, S. E., Jentsch, T. J., and Mathie, A. (1998) *J. Physiol.* **506,** 665–678
38. Ishii, T. M., Silvia, C., Hirschberg, B., Bond, C. T., Adelman, J. P., and Maylie, J. (1997) *Proc. Natl. Acad. Sci. U. S. A.* **94,** 11651–11656
39. Krane, C. M., Melvin, J. E., Nguyen, H. V., Richardson, L., Towne, J. E., Doetschman, T., and Menon, A. G. (2001) *J. Biol. Chem.* **276,** 23413–23420
40. Komwatana, P., Dinudom, A., Young, J. A., and Cook, D. I. (1994) *Pflugers Arch* **428**, 641–647
41. Thiemann, A., Grunder, S., Pusch, M., and Jentsch, T. J. (1992) *Nature* **356,** 57–60
42. Murray, C. B., Morales, M. M., Flotte, T. R., McGrath-Morrow, S. A., Guggino, W. B., and Zeitlin, P. L. (1995) *Am. J. Resp. Cell. Mol. Biol.* **12,** 597–604
43. Blaisdell, C. J., Edmonds, R. D., Wang, X. T., Guggino, S., and Zeitlin, P. L. (2000) *Am. J. Physiol.* **278,** L1248–L1255
44. Rutledge, E., Bianchi, L., Christensen, M., Boehmer, C., Morrison, R., Broslat, A., Beld, A. M., George, A. L., Greenstein, D., and Strange, K. (2001) *Curr. Biol.* **11,** 161–170
45. Nishiyama, A., and Petersen, O. H. (1974) *J. Physiol.* **242,** 173–188
46. Sasaki, T., and Gallacher, D. V. (1990) *FEBS Lett.* **264,** 130–134
47. Foskett, J. K., and Melvin, J. E. (1989) *Science* **244,** 1582–1585
48. Dinudom, A., Young, J. A., and Cook, D. I. (1993) *Pflugers Arch.* **423**, 164–166
49. Dinudom, A., Komwatana, P., Young, J. A., and Cook, D. I. (1995) *J. Physiol.* **487,** 549–555
50. Komwatana, P., Dinudom, A., Young, J. A., and Cook, D. I. (1996) *J. Membr. Biol.* **150,** 133–141
51. Komwatana, P., Dinudom, A., Young, J. A., and Cook, D. I. (1998) *J. Membr. Biol.* **162,** 225–232
52. Zeng, W., Lee, M. G., Yan, M., Diaz, J., Benjamin, I., Marino, C. R., Kopito, R., Freedman, S., Cotton, C., Muallem, S., and Thomas, P. (1997) *Am. J. Physiol.* **273,** C442–C455
53. Lee, M. G., Choi, J. Y., Luo, X., Strickland, E., Thomas, P. J., and Muallem, S. (1999) *J. Biol. Chem.* **274,** 14670–14677